

# Crystal structure of the fission yeast mitochondrial Holliday junction resolvase Ydc2

Simona Ceschini, Anthony Keeley<sup>1</sup>,  
Mark S.B. McAlister<sup>2</sup>, Mark Oram<sup>1</sup>,  
John Phelan<sup>2</sup>, Laurence H. Pearl,  
Irina R. Tsaneva<sup>1</sup> and Tracey E. Barrett<sup>3</sup>

Section of Structural Biology, Institute of Cancer Research,  
Chester Beatty Laboratories, 237 Fulham Road, London SW3 6JB,

<sup>1</sup>Department of Biochemistry and Molecular Biology,  
University College London, Gower Street, London WC1E 6BT,

<sup>2</sup>Department of Crystallography and BBSRC Bloomsbury  
Centre for Structural Biology, Birkbeck College, Malet Street,  
London WC1E 7HX, UK

<sup>3</sup>Corresponding author  
e-mail: barrett@icr.ac.uk

**Resolution of Holliday junctions into separate DNA duplexes requires enzymatic cleavage of an equivalent strand from each contributing duplex at or close to the point of strand exchange. Diverse Holliday junction-resolving enzymes have been identified in bacteria, bacteriophages, archaea and pox viruses, but the only eukaryotic examples identified so far are those from fungal mitochondria. We have now determined the crystal structure of Ydc2 (also known as SpCce1), a Holliday junction resolvase from the fission yeast *Schizosaccharomyces pombe* that is involved in the maintenance of mitochondrial DNA. This first structure of a eukaryotic Holliday junction resolvase confirms a distant evolutionary relationship to the bacterial RuvC family, but reveals structural features which are unique to the eukaryotic enzymes. Detailed analysis of the dimeric structure suggests mechanisms for junction isomerization and communication between the two active sites, and together with site-directed mutagenesis identifies residues involved in catalysis.**

**Keywords:** crystal structure/Holliday junction/  
mitochondrial DNA/resolvase/*Schizosaccharomyces pombe*

## Introduction

Holliday junctions, formed by the reciprocal exchange of strands between two DNA duplexes, occur as intermediates in a variety of genetic processes. These include classical pathways for homologous recombination, double strand break repair and, as shown recently, the rescue and reinitiation of collapsed replication forks (reviewed in Cox *et al.*, 2000; Kowalczykowski, 2000; Michel, 2000) and/or other DNA repair processes during replication (Zou and Rothstein, 1997; Bénard *et al.*, 2001). Resolution of the Holliday junction into two separate duplexes is an essential step in all cases, and is achieved by cleavage of an equivalent strand from each duplex close to the point of

strand exchange by a resolving enzyme. The most extensively characterized mechanism for the processing of Holliday junctions is the RuvABC pathway in *Escherichia coli* and other Gram-negative bacteria (West, 1996). This system utilizes a junction-specific endonuclease, RuvC, that cleaves junctions when a recognition sequence (5' A/T TT↓G/C) is present in both duplexes at or adjacent to the crossover point. The other components of the system, RuvA and RuvB, form a junction-specific helicase or branch migration complex that promotes strand exchange between the linked duplexes and moves the point of crossover.

All prokaryotes have highly conserved homologues of RuvA and RuvB, where RuvA (a Holliday junction 'isomerase') as either a tetramer or octamer distorts the free Holliday junction into an open, square-planar conformation, and RuvB forms an ATP-driven motor facilitating branch migration. There is, however, little or no sequence similarity between and amongst the different groups of junction resolvases. The crystal structures of RuvC (Ariyoshi *et al.*, 1994), T4 endonuclease VII (Raaijmakers *et al.*, 1999), T7 endonuclease I (Hadden *et al.*, 2001) and the archaeal Hjc (Bond *et al.*, 2001; Nishino *et al.*, 2001) have very different folds. Nonetheless, they are all metal ion-dependent endonucleases and seem to have a conserved catalytic mechanism. Recent sequence alignment analyses suggest that RuvC, the A22 pox virus resolvase and the yeast mitochondrial enzymes are related and form a subfamily within the integrase superfamily (Aravind *et al.*, 2000; Garcia *et al.*, 2000; Lilley and White, 2000, 2001). Despite resolvase activities being detected in fractionated extracts of yeast (Parsons and West, 1988) and higher eukaryotes (Constantinou *et al.*, 2001), none have been successfully purified to homogeneity.

The Holliday junction resolvases from *Saccharomyces cerevisiae* (Cce1) and its *Schizosaccharomyces pombe* homologue, Ydc2, play important roles in the maintenance of mitochondrial DNA (mtDNA). *Cce1* mutants show elevated frequencies of petite cells, altered mtDNA transmission patterns and clustering of heritable units (Zweifel and Fangman, 1991; Piskur, 1997). Mitochondrial genome stability may be affected similarly in *S. pombe*, although it may be more difficult to demonstrate in a petite-negative yeast. Both Ydc2 and Cce1 resolve junctions *in vivo*, as shown directly by the accumulation of mtDNA junctions in *cce1 (mgt1)* *S. cerevisiae* mutants (Lockshon *et al.*, 1995) and, similarly, by the dramatic increase in mtDNA aggregation in Ydc2-deficient *S. pombe* cells (Doe *et al.*, 2000). Similar to RuvC, Ydc2 and Cce1 show a marked preference for cleaving four-way junctions (Whitby and Dixon, 1998) after the consensus sequence 5'CT and/or 5'TT in the case of Ydc2 (White and Lilley, 1996; Schofield *et al.*, 1997, 1998; Whitby and

Dixon, 1997, 1998; Oram *et al.*, 1998). Both enzymes distort the stacked-X Holliday junction conformer (which predominates in the presence of divalent metal ions) into a square-planar extended structure, similar to that processed by RuvC (Bennett and West, 1995; White and Lilley, 1997a, 1998).

It has been proposed that several mitochondrial genomes linked via recombination junctions constitute the mtDNA heritable unit in *S.cerevisiae*, whose size is directly affected by the presence of Cce1 (Lockshon *et al.*, 1995). This may be the case in *S.pombe* as the increase in mtDNA aggregation in Ydc2-deficient cells correlates with a reduction in the number of nucleoids (Doe *et al.*, 2000). The resolvase activity of Ydc2/Cce1 is therefore part of the pathway of mtDNA partitioning in yeast cells acting specifically upon junctions formed in some replication-related recombination process, e.g. the initiation of rolling circle replication by homologous recombination. This may be a specialized adaptation of a more general role performed by junction resolvases during DNA replication.

In order to gain further insight into the mechanism of junction isomerization and sequence-specific resolution by these eukaryotic resolvases, we have now determined the crystal structure of the Ydc2 Holliday junction resolvase from the fission yeast *S.pombe*, at 2.3 Å resolution. The structure allows the identification of catalytic residues (which are confirmed by mutagenesis studies), suggests a mechanism for communication between active sites and explains the preference of Ydc2 for binding to Holliday junction substrates in an open conformation.

## Results

### Overall fold

The structure of Ydc2 was determined by single-wavelength anomalous dispersion (SAD) using bacterially expressed recombinant protein, incorporating selenomethionine (see Materials and methods), and refined to 2.3 Å resolution. The structure can be subdivided roughly into two domains, the first consisting of a large  $\beta$ - $\alpha$ - $\beta$  motif (residues 39–241), and the second a smaller helical bundle formed by segments from both the N- (residues 7–38) and C-termini (residues 241–256) (Figure 1A and B). In solution, Ydc2 is dimeric and appears as an intimate dimer in the crystals (see Materials and methods) where the monomers are related by non-crystallographic symmetry (NCS). The overall morphology of the dimer resembles the letter 'S' (Figure 1C) and the interface is formed by the mutual packing of helices 3 and 4 from each monomer. Approximately 1290 Å<sup>2</sup> of solvent-accessible surface is buried on dimer formation that largely derives from the mutual association of hydrophobic patches provided by the side chains of Met137, Met141, Ala144 and Leu145. The strong complementarity of the interface and the high degree of hydrophobic burial suggest that this dimer is biologically authentic.

### Evolutionary relationship to other Holliday junction resolvases

Comparison of the amino acid sequence of Ydc2 with the available protein sequence databases (Altschul *et al.*, 1997) identifies some close yeast and fungal mitochondrial

homologues, including Cce1 and the Mrs1 intron splicing factor (Wardleworth *et al.*, 2000), but does not identify any of the Holliday junction-resolving enzymes previously characterized. Searches starting with the large number of available eubacterial RuvC sequences (Aravind *et al.*, 2000) did unite the Ydc2/Cce1/Mrs1 cluster into a large  $\alpha$ - $\beta$  endonuclease family which includes the bacterial, viral and mitochondrial resolvases, as well as some other nucleases [CATH code: 3.30.420.10 (Pearl *et al.*, 2000); SCOP: RNase H-like superfamily (Murzin *et al.*, 1995)].

The predicted relationship to RuvC is confirmed by comparison of the refined Ydc2 structure with the CATH structural database (Pearl *et al.*, 2000), which identifies the *E.coli* RuvC structure (PDB code: 1HJR) as the most significant match (Figure 2A). Structural alignment of Ydc2 on RuvC using SSAP (Orengo *et al.*, 1992) effectively superimposes strands *a*–*e* of the central  $\beta$ -sheet, helices 3, 4, 5 and 6, and the first two-thirds of helix 8 on equivalent secondary structures in RuvC, with the same topology (Figure 2B). The major difference between the folds occurs in the segment immediately preceding the final helix, which is a seven-residue loop in RuvC, but becomes elaborated into a sixth strand (*f*) of the  $\beta$ -sheet and helix 7, in Ydc2. The small helical domain in Ydc2, formed by helices 1 and 2 and the last third of the C-terminal helix 8, has no equivalent in RuvC. The overall sequence identity between Ydc2 and *E.coli* RuvC on the basis of this structural alignment is <10%. The sequence identity between Ydc2 and Cce1 is ~21% although Ydc2 is nearly 80 residues shorter. The additional residues in Cce1 are accommodated in more extensive loops existing between helices 1 and 2, 5 and 6, 6 and 7, and 7 and 8, as well as an extension of ~30 residues at the C-terminus. Relatively few insertions occur in the remainder of the structure that comprises the central  $\beta$ -sheet, and helices 3 and 4 that form the dimer interface.

### Active site location and catalytic residues.

Proteins that have evolved to interact with nucleic acids are found typically to display an anisotropic distribution of charged amino acids. This generates a strong dipole moment across the protein molecule, which promotes high affinity for the negatively charged nucleic acid backbone when presented in a favourable orientation. As expected, calculation of the surface electrostatic potential of the Ydc2 dimer shows a very marked anisotropy, with one face of the flattened 'S' structure displaying a considerable degree of positive potential (Figure 3A). These regions are centred on the small helical bundle domain, and on the loops connecting helices 5 and 6, helices 7 and 8, and strand *d* with helix 4, which protrude from the surface of this face. In contrast to the predominantly positively charged face in Ydc2, which is presumed to be involved in DNA binding, the base of the valley between the strand *d*-helix 4 and helix 5-helix 6 loops displays an intense negative potential. This negatively charged patch is generated by a cluster of acidic residues originating from the C-terminal ends of strands *a* (Asp46) and *d* (Glu117), in addition to the N-terminus of helix 8 (Asp226, Asp227 and Asp230). These residues are conserved in Cce1 and, in the structure-based alignment with RuvC (the exception being Asp226 in Ydc2), correspond to a conserved acidic cluster (Ariyoshi *et al.*, 1994) (Figure 3B). Within this

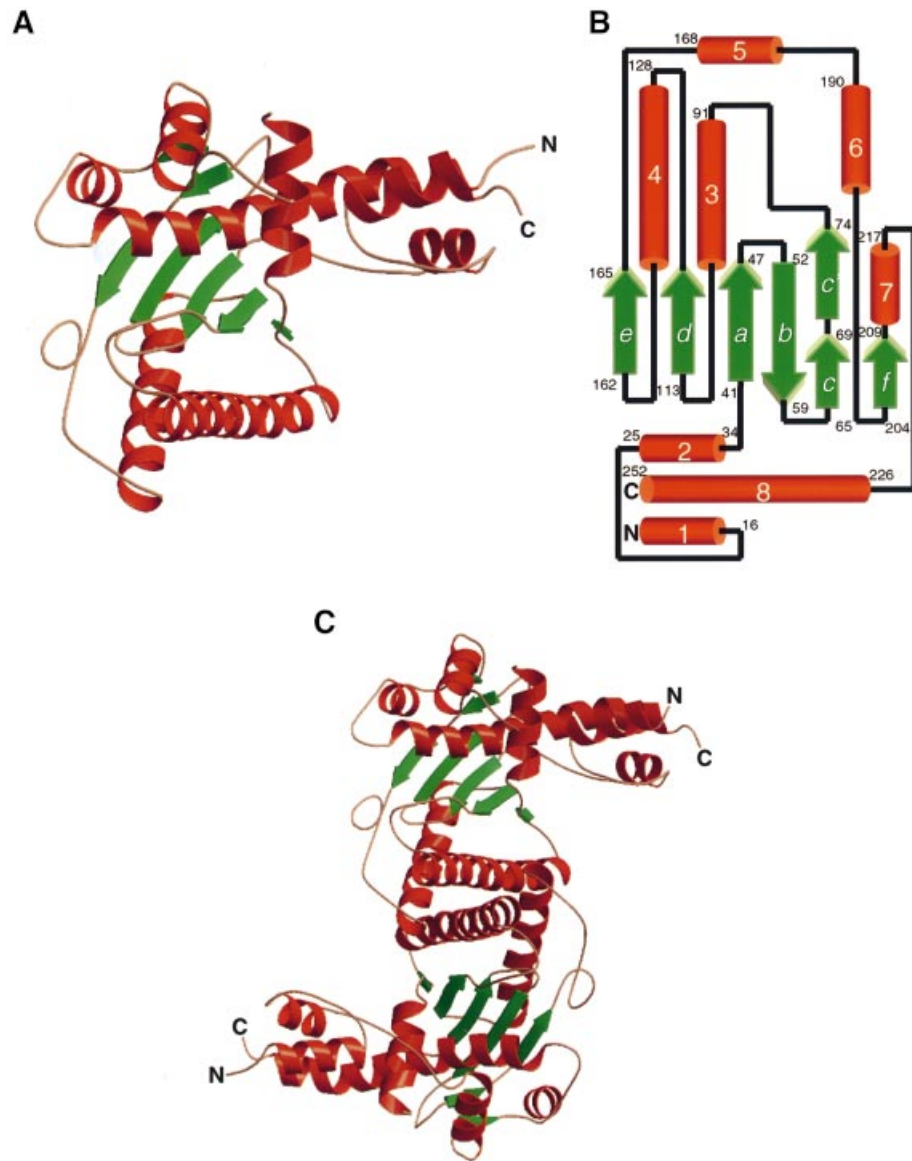


**Fig. 1.** Ydc2 structure. (A) Secondary structure cartoon of the Ydc2 monomer. This and other molecular graphics figures were generated using Bobscript (Robert Esnouf's adaptation of Molscript; Kraulis, 1991) and rendered using RASTER3D (Merrit and Murphy, 1994), except for Figures 3A and 7B, which were generated using GRASP (Nicholls *et al.*, 1993). (B) Topology of the secondary structural elements. (C) Secondary structure cartoon of the Ydc2 dimer observed in the crystals, viewed down the non-crystallographic 2-fold axis. The significant surface area burial and conservation of the interface suggest that this is the biologically authentic dimer.

cluster in RuvC, Asp7 and Asp141 were shown to bind  $Mn^{2+}$  ions in soaked crystals, and mutation of either caused complete loss of nuclease activity, but not junction binding (Ichianagi *et al.*, 1998). Taken together with the dependence of the nuclease activity of RuvC on  $Mg^{2+}$  (Bennett *et al.*, 1993; Takahagi *et al.*, 1994), these data implicate Asp7 and Asp141 as the binding sites for catalytic  $Mg^{2+}$  ion(s). In one of the monomers forming the asymmetric unit in the Ydc2 structure, difference Fourier maps in the vicinity of this cluster show an electron density feature consistent with a single bound metal ion close to the carboxylate side chains of Asp46, Asp230 and Glu117, which are topologically equivalent to Asp7, Asp141 and Glu66 of RuvC (Figure 4A). Additional ligands to the putative metal are provided by the hydroxyl group of Tyr172 and the peptide carbonyl of Arg118. This

coordination is more commonly associated with  $Ca^{2+}$  ions although none were included explicitly in the buffers used for protein purification or crystallization. Consistent with essential roles in the chelation of catalytic metal ions, site-directed mutation of either Asp230 or Asp46 in Ydc2 to asparagine resulted in total loss of Holliday junction cleavage activity even in the presence of high concentrations of  $Mg^{2+}$ , although both mutants retained wild-type binding affinity for Holliday junctions (Figure 4B and C).

In a previous mutagenesis study of Cce1 (Wardleworth *et al.*, 2000), two other acidic residues (Asp293 and Asp294) were identified as essential for  $Mg^{2+}$  binding and, consequently, for catalytic activity. Although the corresponding residues in the Ydc2 structure (Asp226 and Asp227) are close to the putative metal site, they are

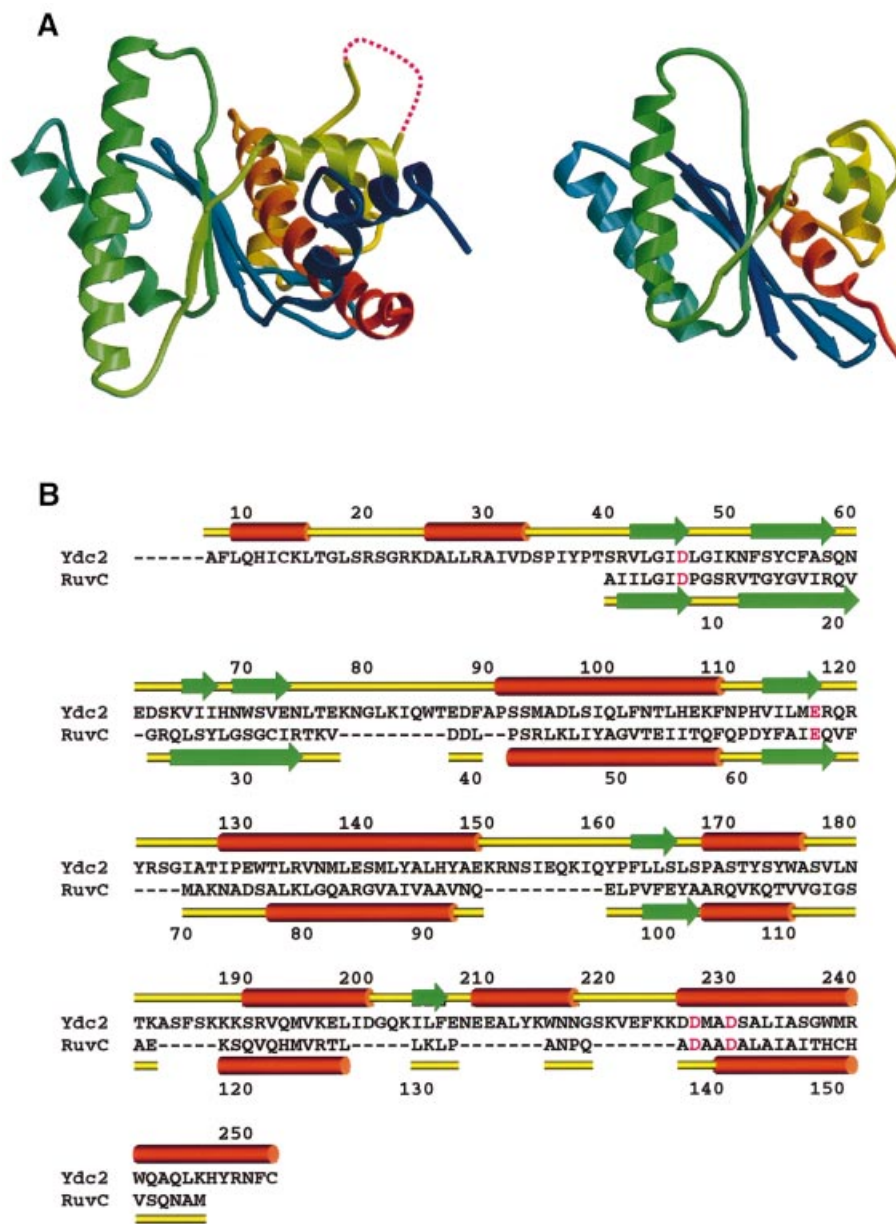


**Fig. 2.** Structural homology of Ydc2 and RuvC. (A) Secondary structure cartoons of Ydc2 (left) and *E. coli* RuvC (right) colour-ramped blue→red from the N- to C-termini. The structures were superimposed using SSAP (Orengo *et al.*, 1992) and separated for clarity. (B) Structure-based sequence alignment of Ydc2 and *E. coli* RuvC. Residues implicated in catalysis and conserved between Ydc2 and RuvC are highlighted in magenta.

unfavourably positioned to make direct contact, but are linked to the direct metal ligands. Thus, the peptide carbonyl oxygen of Asp226 is hydrogen bonded to the peptide nitrogen of Asp230, one turn along in helix 8, and Asp227 on the same helix makes a side chain hydrogen bond to Asn51 on the  $\beta$ -hairpin that carries Asp46. Therefore, mutations in Asp226 and/or Asp227 that have the potential to cause shifts in their interactions and position may achieve some of their effect on  $Mg^{2+}$  binding indirectly by creating shifts in the positions of the direct ligands Asp46, Asp230 and Glu117 to which they are coupled conformationally. In addition, the reduction in negative electrostatic potential that would result from mutation of the carboxylate side chain could significantly destabilize the binding of cations. It is worth noting that Tyr172 is replaced by threonine in Cce1, which, although

capable of similar interactions with a metal ion, would be at an inappropriate distance from the binding site without remodelling of the region.

Other residues mutated in Cce1 that produced either loss of catalysis or a reduction in junction binding include the residues equivalent to Phe52, Arg118, Gln119, Arg191 and Lys225 in Ydc2. The mutation of Phe52 to alanine results in a 200-fold reduction in activity and also a decrease in binding affinity. It is clear from the Ydc2 structure that this residue is buried in the hydrophobic core of the protein and is incapable of having any direct role in interacting with a Holliday junction. Destabilization of the protein structure or disruption of its folding pathway are probably the most likely explanations for the loss of function associated with this mutation. Similar reductions in binding affinity have also been observed for mutants of

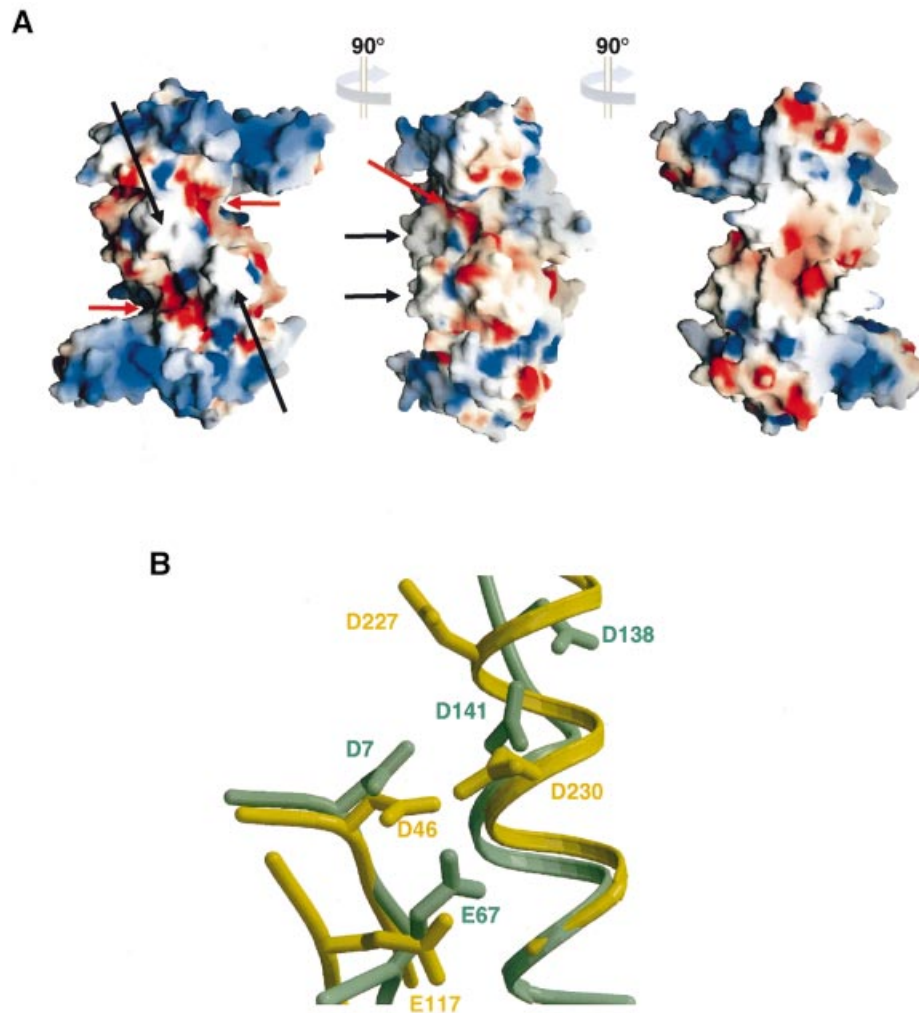


**Fig. 3.** DNA-binding surface and active site of Ydc2. **(A)** Orthogonal views of the molecular surface of the Ydc2 dimer coloured (blue→red, +ve→-ve) according to electrostatic potential. One face (left) shows a substantial excess of basic residues consistent with DNA binding, whilst the recessed negative patches are formed by a cluster of conserved acidic residues (red arrows). The 'pin' segments connecting strand *d* and helix 4 protrude from this face (black arrows). The opposite face (right) has a more acidic surface. **(B)** Conserved residues forming the acidic patch from Ydc2 (yellow) structurally aligned with the topologically equivalent residues from RuvC (green). Mutagenesis and crystallographic studies of RuvC implicate Asp7 and Asp141 as essential ligands for a catalytic metal ion.

Arg191 and Lys225. Both are located close to the catalytic centre at the C-terminal ends of helices 6 and 8, respectively, and are therefore likely to have roles in Holliday junction binding via interactions with phosphate groups. Consistent with this, electron density for single sulfate ions associated with the guanidinium head groups of Arg191 in both monomers has been observed. Residues Arg118 and Gln119 are positioned adjacent to Glu117, which is a direct ligand of the bound metal ion in Ydc2 and probably has an important role in catalysis. Any mutations in this region are therefore likely to alter the environment of Glu117, resulting in reduced hydrolytic activity and diminished binding affinity due to remodelling of the flexible 117–128 loop.

#### **Conformational flexibility in the Ydc2 dimer**

Comparison of the two molecules forming the crystallographic asymmetric unit reveals a number of regions within Ydc2 that appear capable of undergoing significant movement. Of particular interest are the conformational

differences that occur in the active site involving helix 5,  $\beta$ -strand *d* and the side chain of Asp230 (Figure 5A). In one monomer, residues Asp230, Asp46, Glu117 and Tyr172 are liganded directly to a putative metal ion, as described above. In the second monomer, this site is substantially rearranged. Asp230 adopts a different rotamer that directs it away from the metal-binding site. In addition, movements in helix 5 of  $\sim 5$  Å together with substantial remodelling of  $\beta$ -strand *d* result in the side chains of Glu117 and Tyr172 also being directed away from the metal-binding site. The largest movement involves Tyr172, which rotates  $\sim 180^\circ$  from its position in the first monomer and becomes directed towards the solvent. These differences in conformation completely disrupt the interactions observed with the metal ion in the first monomer, and no electron density for a bound metal is present in the second.

Changes in conformation are also apparent in the loop spanning residues 59–62, helix 4, which forms part of the dimer interface, and the side chains of residues 230 and

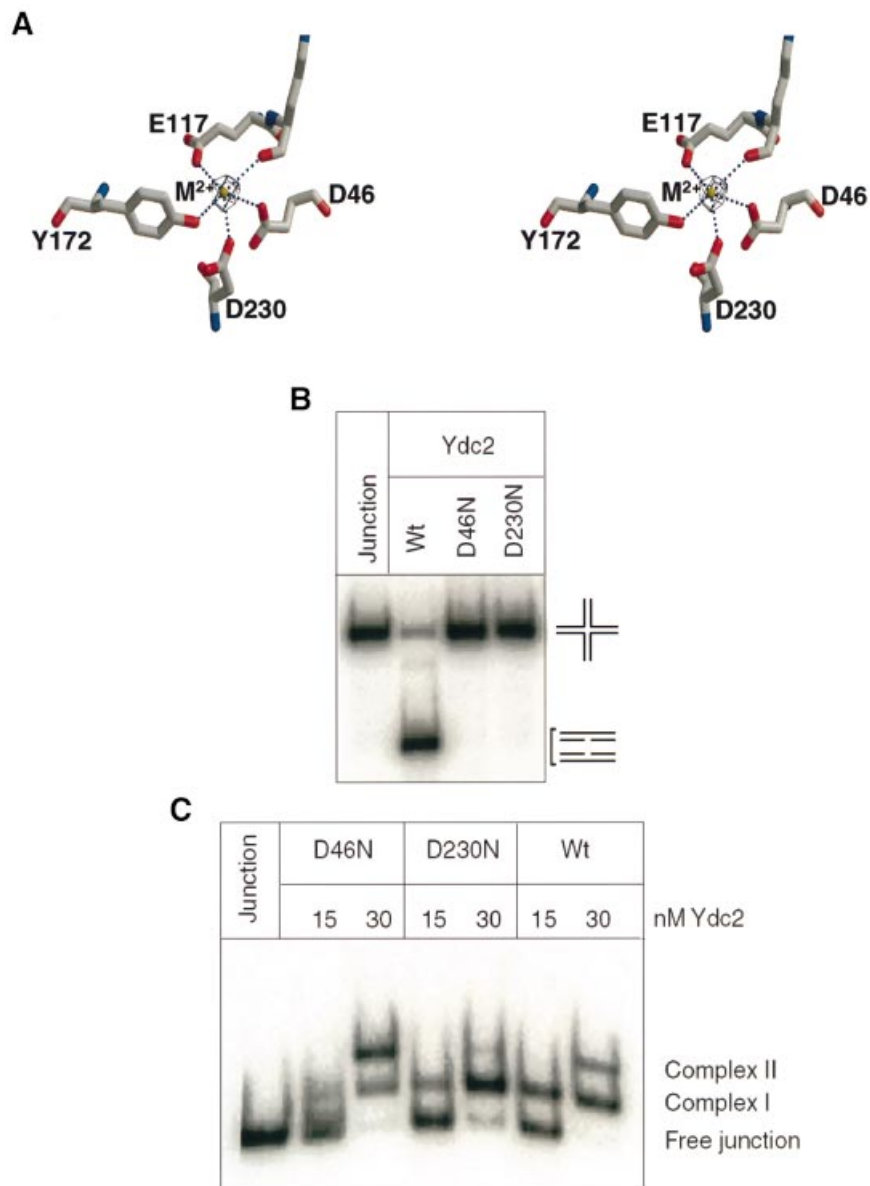


**Fig. 4.** Identification and mutagenesis of catalytic residues. (A) Bound metal ion observed in one Ydc2 monomer. The coordination is most consistent with a calcium ion, but the site would probably accommodate two  $Mg^{2+}$  ions during catalysis. The electron density shown is from an  $F_o - F_c$  map contoured at  $2.5\sigma$ . (B) Mutation of either of the direct metal ligands Asp46 or Asp230 to asparagine completely abolishes the ability of Ydc2 to resolve Holliday junctions in the presence of  $Mg^{2+}$ , compared with the wild-type enzyme, which efficiently releases nicked duplexes under the same reaction conditions. (C) Both mutants and the wild-type enzyme are able to bind to Holliday junctions in the absence of  $Mg^{2+}$ , implying purely catalytic roles for Asp46 and Asp230.

223. In addition, residues 22–25, 122–129, 181–189 and 220 become disordered in the metal-free monomer. Residues 153–159 and 181–186 are disordered in the metal-bound monomer. With the exception of residues 59–62, all of these regions are located at or close to the surface of the Ydc2 dimer and map to the positively charged face presumed to associate with the Holliday junction. It is likely that these segments of polypeptide are involved in substrate recognition and may undergo significant rearrangements in order to facilitate junction binding. In the metal-bound monomer, residues 118–128 form part of a ‘pin’ anchored by strand *d* and helix 4 at the N- and C-termini, respectively. The latter part of the loop (residues Ser123–Ile128) is involved in crystal contacts,

which would certainly contribute to the ordering of this region compared with the metal-free monomer. These interactions, however, are  $>18$  Å distant from Glu117 and are therefore unlikely to be responsible for the conformational differences observed. The sensitivity of Cce1 activity to mutations of the equivalent residues to Arg118 or Gln119 suggests that the ‘pin’ may play a role in correctly positioning Glu117 for catalysis. Variations in the conformation of the active site are transmitted via Glu117 and influence the conformation and order of the ‘pin’ segment. Changes in ‘pin’ conformation would then be communicated to the other monomer via helix 4, which is directly involved in formation of the dimer interface.

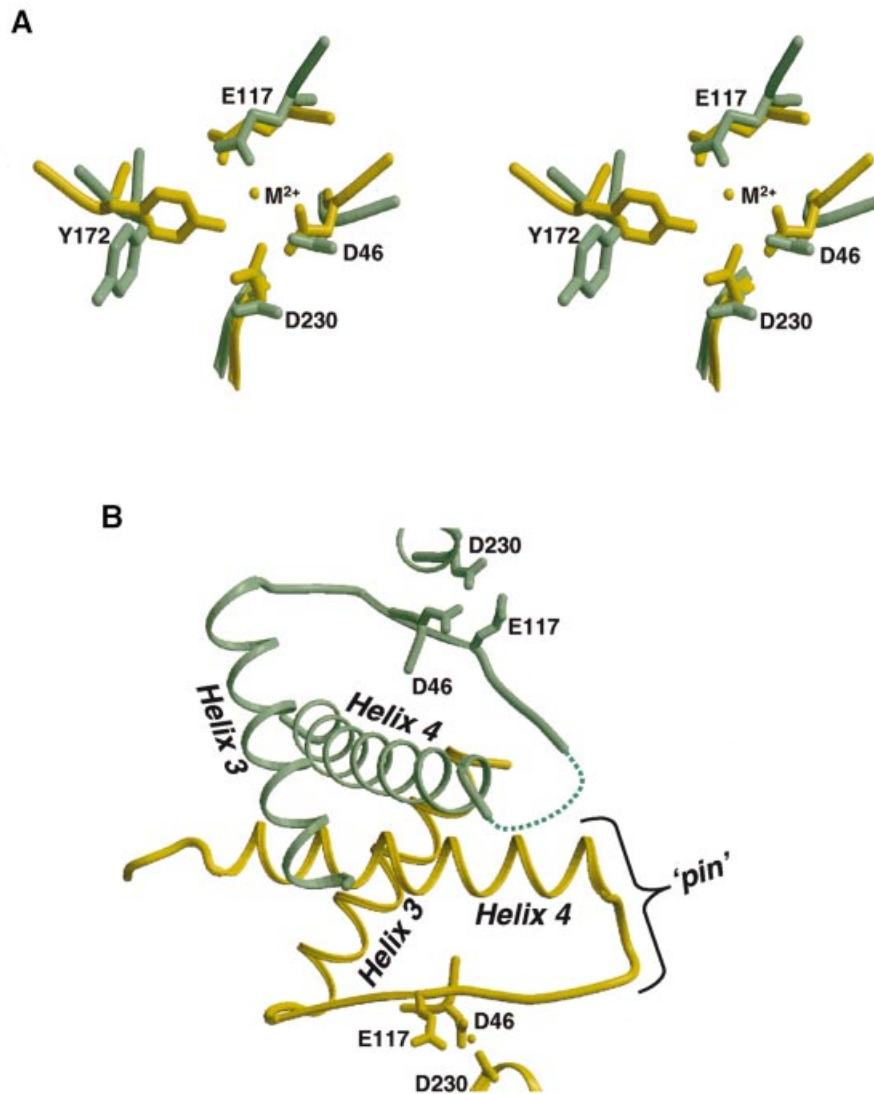


**Fig. 5.** Active site variability and communication. (A) Superposition of the active sites from the metal-ion bound monomer (yellow) and the metal-free monomer (green). Significant changes in conformation of side chains and in the order of adjacent segments of the polypeptide chain occur as a result of metal ion binding. (B) A pathway for communication between the two active sites is provided by the direct interaction of the N-termini of helix 4 at the dimer interface. These are directly linked to the flexible 'pin' segments, which in turn connect to the active site metal ion ligand Glu117. Changes in the conformation of one active site would be communicated to the other site via this pathway, and could mediate the positive cooperativity observed between the first and second strand cleavage reactions.

### Model for junction binding

The four-way DNA Holliday junctions recognized and cleaved by Holliday junction resolvases can exist in two interchangeable but distinct three-dimensional structures (reviewed in Duckett *et al.*, 1995; Lilley and Norman, 1999). In the folded state (Ortiz-Lombardia *et al.*, 1999), the two strand-swapped duplexes traverse each other at an acute angle, in a so-called 'stacked-X' structure where one strand (continuous) from each duplex remains more or less co-linear with the helix axis. The complementary (discontinuous) strand reverses direction as it invades the homologous duplex. In the open state, observed in complexes with RuvA tetramers or octamers (Hargreaves *et al.*, 1998; Roe *et al.*, 1998; Ariyoshi *et al.*, 2000), the Holliday junction has an approximately square-planar structure in which all four arms are equivalent, with no distinction between continuous and discontinuous strands. The presentation of the sugar-phosphate backbone is

sufficiently different between these two states that interacting proteins inevitably are committed evolutionarily to preferential interaction with one or the other, and may thereby promote their interconversion.

Biochemical data for Cce1 and Ydc2 binding to Holliday junctions suggest a strong preference for binding to an open rather than folded conformation and an ability to promote unfolding of stacked-X structures (White and Lilley, 1997b, 1998; White *et al.*, 1997; Kvaratskhelia *et al.*, 1999), in a similar way to the bacterial RuvA and the proposed RuvABC complex (Bennett and West, 1995; Parsons *et al.*, 1995; Whitby *et al.*, 1996; Eggleston *et al.*, 1997). Preferential cleavage of a bound Holliday junction by Ydc2 occurs on opposite strands of the phosphodiester bonds at, or adjacent to, the point of strand crossover. The distance between the pair of scissile bonds in a Holliday junction with an open square-planar structure (Roe *et al.*, 1998) is ~30–35 Å. In an antiparallel stacked-X structure

(Ortiz-Lombardia *et al.*, 1999), the scissile bonds in the continuous strands are also separated by  $\sim 30\text{--}35$  Å, but this can be reduced substantially for the discontinuous strands. The observed distance between the putative metal sites in the Ydc2 dimer is  $\sim 34$  Å, allowing simultaneous interaction with symmetry-equivalent bonds in the DNA backbone either in an open square-planar conformation or with the continuous strands in a stacked-X conformation. However, binding of the stacked-X conformation would generate a substantial steric clash between the points of crossover at the centre of the folded Holliday junction and the 'pin' (see above) at the dimer interface. In the square-planar conformation, these central protrusions are accommodated by the central hole. A model Holliday junction in the open square-planar conformation can thus be docked against the positively charged surface of the Ydc2 dimer with no significant steric clashes with the protein, such that both scissile bonds are simultaneously within  $\sim 6$  Å of the putative active sites (Figure 6). In this modelled complex, the major groove in each arm of the junction is directed away from the protein surface and fully exposed, consistent with methylation protection studies of Ydc2 (White and Lilley, 1998). Two opposing arms in the square-planar Holliday junction in this modelled complex come into close contact with the positively charged surface of the triple-helix domains, disposed on either side of the Ydc2 dimer. A plethora of lysine and arginine side chains extend from this surface and could make extensive ionic and hydrogen-bonding interactions with the negatively charged sugar-phosphate backbone of the DNA in these arms of the junction, providing a platform that supports the open unstacked conformation.

## Discussion

The crystal structure of Ydc2 confirms the prediction that the mitochondrial resolvases are evolutionarily related to the RuvC family of resolving enzymes, although they exhibit almost undetectable similarity at the sequence level. There are, however, distinct structural differences between Ydc2 and RuvC, most notably the triple-helix domain in Ydc2, which is formed by N- and C-terminal extensions to the conserved core fold. Structural alignment of Ydc2 with bacterial RuvC implicates Asp46 and Asp230 as catalytic residues rather than Asp226 and Asp227 as suggested by earlier mutagenesis studies (Wardleworth *et al.*, 2000), and the carboxylates of Asp46 and Asp230 are in direct contact with a bound metal ion in one monomer of the Ydc2 structure. Consistent with a role in catalysis, D46N and D230N Ydc2 mutants retain junction-binding activity, but fail to cleave. In the crystals, only one of the putative active sites in the dimer is occupied by a metal ion, and comparison of the two monomers reveals conformational differences between the catalytic groups in the metal-bound and free monomers that are directly connected to the helices forming the 'pin' structure at the dimer interface. The coupling of active site conformation to the dimer interface is particularly interesting, and may play a role in the positive cooperativity observed between the first and second cleavage reactions (Fogg *et al.*, 2000). Thus, following the first cleavage, conformational changes within the active site of the first monomer could result in

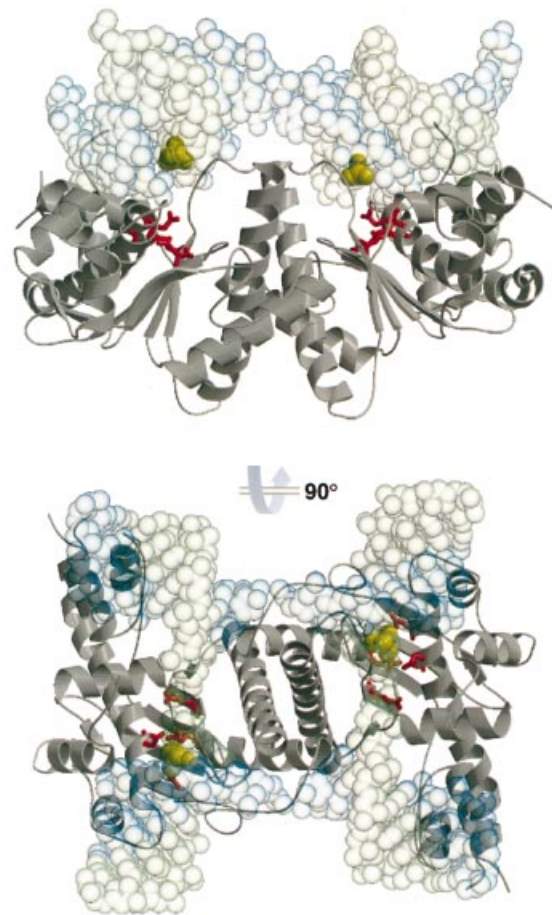


**Fig. 6.** Holliday junction complex. Model of a productive Ydc2–Holliday junction complex. A model Holliday junction in an open, approximately square-planar conformation (transparent CPK model) can be docked onto the basic face of the Ydc2 dimer, bringing the scissile phosphodiester bonds close to the acidic cluster and the metal ion-binding site (red). The 'pin' and N-terminus of helix 4 that protrude from this face are accommodated by the centre of the open junction, but would prevent binding of the junction in a stacked-X conformation. Scissile phosphate groups are highlighted in yellow.

ejection of the metal ion(s) and trigger movements in helix 4 of the dimer interface via the 118–128 loop. These motions could be relayed to the catalytic residues of the second monomer and promote optimal positioning for metal ion binding and subsequent catalysis, possibly assisted by changes in the Holliday junction structure itself resulting from the initial incision (Figure 5B).

The positions of the catalytic site and putative metal ion, in conjunction with the distinctive positive potential and 'pin' structure on one face of the dimer, have enabled us to construct a plausible model for a productive Ydc2–Holliday junction complex based on a square-planar extended junction conformation. In this model, the triple-helix domains mediate a considerable number of interactions involving lysines/arginines and phosphate groups and may therefore have essential roles in substrate recognition. The 'pin' structure at the dimer interface protrudes into the centre of the open junction, and may play a role in mediating the observed specificity for the sequence in the vicinity of the point of strand crossover.

The addition of the highly basic triple-helix domain significantly alters the overall shape of the Ydc2 dimer as

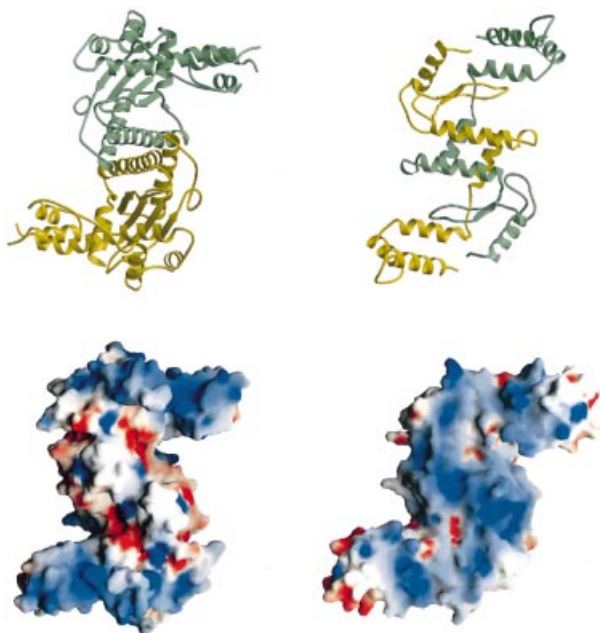


**Fig. 7.** Convergent 'S'-shaped structures for Ydc2 and T4 endo VII. Ydc2 (left) and bacteriophage T4 endo VII (right) show a remarkable similarity in their overall shape, despite totally unrelated architectures and folds. Both have an 'S' shape when viewed towards their basic DNA-binding surfaces, and both have basic triple-helix domains extending out from their core. However, they have very different specificity for the conformation of their Holliday junction substrate.

compared with the RuvC structure, generating an 'S'-shaped structure with a distinctive positive potential over one face. Although entirely unrelated in sequence or polypeptide fold, an 'S'-shaped structure has also been observed for the bacteriophage Holliday junction resolvase, T4 endo VII (Raaijmakers *et al.*, 1999). In both cases, one face of the dimer displays a significantly basic character consistent with a role in DNA binding, and defines the 'hand' of both structures as 'S' shaped rather than 'Z' shaped. The putative active sites in both Ydc2 and T4 endo VII occur close to the 'elbow' between the central dimerized domain and laterally protruding triple-helix domain. However, the inter-site spacing is significantly shorter in the case of T4 endo VII, reflecting its preference for cleavage of a stacked-X Holliday junction conformation, rather than the open structure promoted by Ydc2 (Figure 7).

In the context of a RuvABC complex, the activity of RuvC is functionally coupled to RuvA, which manipulates the junction into the extended conformation observed in the RuvA-Holliday junction complex structures (Hargreaves *et al.*, 1998; Roe *et al.*, 1998; Ariyoshi *et al.*, 2000). The yeast mitochondrial enzymes Cce1 and Ydc2 seem to have no requirement for a separate junction isomerase protein, and are able to induce an extended conformation themselves, even in the presence of high concentrations of divalent metal ions. By opening the stacked-X junction, they may achieve some degree of short-range 'scanning' to locate their specific sequences close to the crossover point. An interesting prospect is that Ydc2/Cce1 may operate as a functional fusion of RuvC and RuvA, thus preparing the junction for branch migration. Long-range scanning, if a biological requisite, must

still be presumed to depend on an active ATP-dependent helicase partner, analogous to the bacterial RuvB, which is at present unknown. In budding yeast cells, Cce1 is found to be associated with the mitochondrial inner membrane (Ezekiel and Zassenhaus, 1993), presenting the problem of how the enzyme finds its substrates. One possibility is that all junctions are formed and processed at replication/

repair 'factories' at the inner mitochondrial membrane. Alternatively, there may be some active mechanism of junction translocation, analogous to branch migration. This would ensure a system of delivering the junctions to Ydc2/Cce1 and at the same time would address the problem of junctions formed at uncleavable sequences.

## Materials and methods

### Cloning, expression and purification

The expression plasmid pET-Ydc2 contained the Ydc2 open reading frame (ORF) cloned in the *Nde*I-*Xho*I sites of the pET21a(+) vector (Oram *et al.*, 1998). The Ydc2-His expression construct (pET-Ydc2-His) was generated by mutating the 3' end of the cloned sequence in plasmid pET-Ydc2 containing the natural stop codon and the *Xho*I cloning site (TAGTCTCGAG), to TATCGCGAG, using the Quick Change<sup>®</sup> system (Stratagene). This extended the Ydc2 ORF by two extra amino acid residues (tyrosine and arginine) in-frame with the C-terminal His<sub>6</sub> tag in the pET21a(+) vector.

*Escherichia coli* BL21 (DE3) cells (Novagen) transformed with pET21a-Ydc2 were grown at 37°C in LB supplemented with 100 µg/ml ampicillin to an OD<sub>600 nm</sub> of 0.8, before induction with 0.1 mM isopropyl-β-D-thiogalactopyranoside (IPTG). Cultures were incubated for a further 3–4 h, before harvesting by centrifugation at 2000 *g* for 15 min. Cell pellets were resuspended in 20 ml of buffer A (50 mM Tris NaH<sub>2</sub>PO<sub>4</sub>, 15 mM imidazole, 1 M NaCl pH 7.5) per litre of original culture and stored at –80°C. For biosynthetic labelling of Ydc2 with seleno-L-methionine (Se-Met), BL21 or B834 (DE3) cells transformed with pET21a-Ydc2 were grown at 30°C in minimal medium supplemented with 0.8 mM Se-Met, and induced under the same growth conditions. DNase I (10 µg/ml) and a protease inhibitor cocktail (Boehringer Mannheim) were added to the thawed cell suspension before disruption by sonication on ice. Cell lysates were clarified by centrifugation at 40 000 *g* and loaded onto Ni-NTA (Qiagen) or Talon columns (5 × 1.6 cm) equilibrated in buffer A. This was followed by washing with 100 ml of buffer A and then 100 ml of buffer B (buffer A with 50 mM imidazole pH 7.5), before elution with 100 ml of buffer C (buffer A with 500 mM imidazole pH 7.5). The Ydc2 pool was buffer-exchanged immediately by gel filtration using a Sephadex G25 column (10 × 1.6 cm), pre-equilibrated in 50 mM Tris, 1 M NaCl, 5% (w/v) glycerol pH 8 and eluted at 2 ml/min. This step was necessary to reduce time-dependent precipitation of Ydc2. All fractions were analysed by Tris-tricine SDS-PAGE and were essentially pure by visual inspection. The buffer-exchanged Ydc2 pool was then concentrated by ultrafiltration using a centrifugal concentrator (10 kDa NMWL) (Vivascience) to 10 mg/ml and used in protein crystallization trials. Se-Met-labelled samples were also purified using the above procedure.

### Crystallization and data collection

Crystals of the native protein were grown using the microbatch crystallization technique from the following conditions: 2.0 M ammonium sulfate/dihydrogen phosphate, 0.1 M sodium acetate pH 4.6/0.1 M Tris-HCl pH 8.5. Crystals were also obtained from 0.5 M lithium sulfate monohydrate and 15% (w/v) polyethylene glycol 8000. Se-Met-substituted crystals could only be obtained from 2.0 M ammonium sulfate/dihydrogen phosphate, 0.1 M sodium acetate pH 4.6/0.1 M Tris-HCl pH 8.5 after streak seeding. All crystals were orthorhombic; however, four distinct but related forms were identified, of which two were used for structure determination and refinement (forms 1 and 2, see Table I). Crystal volume calculations indicated that both forms contained two molecules in the asymmetric unit. A significant (40σ) peak at  $u = 0.055$ ,  $v = 0.00$ ,  $w = 0.5$  in native Patterson functions calculated for form 1 suggested that the two independent molecules were related by a non-crystallographic translation. Systematic absences in form 1 were

**Table I.** Crystallographic data

Crystal	Se-Met (form 1), Native (form 2) $\lambda = 0.9796$	
Space group	$P2_12_12_1$	$P2_12_12_1$
Unit cell	$a = 74.74$ $b = 133.37$ $c = 77.23$	$a = 72.00$ $b = 133.94$ $c = 73.25$
No. of molecules/asymmetric unit	2	2
Solvent content (%)	58	54
Resolution (Å)	30–2.85	30–2.3
No. of unique reflections	18 530	31 239
Completeness (%)	99.3	91.9
Multiplicity	4.0	3.4
$R_{\text{merge}}$ (%) (outer)	0.048 (0.162)	0.034 (0.219)
$I/\sigma(I)$	8.8 (2.6)	16.0 (3.6)
<FOM> (from SOLVE)	0.34 (0.24)	
Refinement statistics (crystal form 2)		
Resolution (Å)	30–2.3	
No. of protein atoms	3749	
No. of water molecules	222	
No. of sulfate ions	2	
$R_{\text{free}}$	0.270	
$R_{\text{cryst}}$	0.238	

ambiguous and it was impossible to distinguish between  $P2_12_12_1$  or  $P2_12_12_1$ . Significant differences in the cell dimensions of form 2 relative to form 1 were observed, particularly in the length of the  $c$ -axis, which decreased by up to 4 Å. Unlike form 1, there was no convincing evidence of a non-origin peak in native Patterson functions, and systematic absences along the  $c$ -axis indicated the space group to be  $P2_12_12_1$ .

### Structure determination and refinement

The structure of Ydc2 was solved using the Se-Met SAD technique with peak wavelength data collected at the ESRF on beamline ID14-4. Diffraction data were collected on a single Se-Met-substituted crystal (form 1) at 100 K and processed using DENZO (Otwinowski and Minor, 1993) and SCALA (CCP4, 1994) to 2.85 Å. A full three-wavelength multiwavelength amorphous dispersion (MAD) experiment was performed, but remote and inflection point data had to be excluded due to considerable radiation damage. Ten out of the possible 14 Se atoms in the asymmetric unit were identified using SOLVE (Terwilliger and Berendzen, 1999) with calculations executed in space group  $P2_12_12_1$  and the resultant preliminary phases improved using RESOLVE (Terwilliger, 2000). The initial map calculated from the RESOLVE phases was readily interpretable and it was possible to assign ~60% of the total structure including side chains of a single monomer using O (Jones *et al.*, 1991) (the remaining monomer was generated by application of the NCS operator). This partial structure was refined using CNS (Brünger *et al.*, 1998) and the coordinates used as a molecular replacement search model in AmoRe (Navaza, 1994) to determine the orientation and position of the two Ydc2 molecules within the form 2 unit cell where data were available to higher resolution (2.3 Å). The highest peaks were obtained when the translation function was performed in  $P2_12_12_1$ , confirming it as the correct space group. The correctly positioned molecules were subjected to cycles of refinement and manual rebuilding until the entire sequence could be placed with the exception of disordered loops and some solvent-exposed side chains. Initially, all modifications were made to one monomer and the NCS operator used to generate the second; however, in later cycles, both molecules were refined and rebuilt independently. The current model consists of 3749 protein atoms, 222 water molecules and two sulfate ions, with geometric parameters well within the expected ranges for structures at this resolution (Laskowski, 1993). Coordinates for the refined structure have been deposited in the Protein Databank with accession code 1KCF.

### Mutagenesis

Mutations of Asp46 and Asp230 to asparagine were engineered using the Quick Change® site-directed mutagenesis kit from Stratagene and were

verified by sequencing. The two mutant proteins were overexpressed and purified as for wild-type Ydc2.

Junction resolvase activity was assayed using a synthetic four-way junction X12, end-labelled with  $^{32}\text{P}$  in strand 1, as previously described (Oram *et al.*, 1998). Reaction mixtures contained ~5 ng of X12 DNA in 50 mM Tris-HCl pH 8.0, 10 mM  $\text{MgCl}_2$ , 50 mM KCl, 1 mM dithiothreitol (DTT) and 100 µg/ml bovine serum albumin (BSA), and the indicated amount of Ydc2 (expressed as monomers of protein). The reactions were analysed by 6% neutral PAGE and visualized using a Fujifilm FLA-2000 phosphorimager. Binding reactions were performed in 50 mM Tris-HCl pH 8.0, 200 mM NaCl, 5 mM EDTA, 1 mM DTT, 100 µg/ml BSA. The reactions contained 5 ng of  $^{32}\text{P}$ -labelled synthetic junction and varying concentrations of Ydc2. Proteins were diluted in 20 mM Tris-HCl pH 7.5, 150 mM NaCl, 1 mM EDTA, 0.5 mM DTT, 100 µg/ml BSA and 10% glycerol. Incubation was for 15 min on ice and samples were loaded directly onto 6% polyacrylamide gels in TBE buffer. Electrophoresis was performed at 10 V/cm at 4°C with continuous buffer recirculation. Gels were dried and bands visualized using a Fujifilm FLA-2000 phosphorimager.

### Acknowledgements

We are very grateful to our colleagues Mark Roe and David Barford for assistance with data collection, and to the ESRF, Elettra and Daresbury synchrotrons for beam time. We gratefully acknowledge the financial support of the Wellcome Trust (I.R.T.), Cancer Research Campaign (T.E.B. and L.H.P.), Institute of Cancer Research Structural Biology Initiative (L.H.P. and T.E.B.) and the BBSRC Bloomsbury Centre for Structural Biology. I.R.T. is a Wellcome Trust Senior Research Fellow. T.E.B. is a BBSRC David Phillips Research Fellow.

### References

- Altschul,S.F., Madden,T.L., Schäffer,A.A., Zhang,J., Zhang,Z., Miller,W. and Lipman,D.J. (1997) Gapped BLAST and PSI-BLAST: a new generation of protein database search program. *Nucleic Acids Res.*, **25**, 3389–3402.
- Aravind,L., Makarova,K.S. and Koonin,E.V. (2000) Holliday junction resolvases and related nucleases: identification of new families, phyletic distribution and evolutionary trajectories. *Nucleic Acids Res.*, **28**, 3417–3432.
- Ariyoshi,M., Vassilyev,D.G., Iwasaki,H., Nakamura,H., Shinagawa,H. and Morikawa,K. (1994) Atomic-structure of the RuvC resolvase—a Holliday junction-specific endonuclease from *Escherichia coli*. *Cell*, **78**, 1063–1072.
- Ariyoshi,M., Nishino,T., Iwasaki,H., Shinagawa,H. and Morikawa,K. (2000) Crystal structure of the Holliday junction DNA in complex with a single RuvA tetramer. *Proc. Natl Acad. Sci. USA*, **97**, 8257–8262.
- Bénard,M., Maric,C. and Pierron,G. (2001) DNA replication-dependent formation of joint DNA molecules in *Physarum polycephalum*. *Mol. Cell*, **7**, 971–980.
- Bennett,R.J. and West,S.C. (1995) Structural analysis of the RuvC–Holliday junction complex reveals an unfolded junction. *J. Mol. Biol.*, **252**, 213–226.
- Bennett,R.J., Dunderdale,H.J. and West,S.C. (1993) Resolution of Holliday junctions by RuvC resolvase: cleavage specificity and DNA distortion. *Cell*, **74**, 1021–1031.
- Bond,C.S., Kvaratskhelia,M., Richard,D., White,M.F. and Hunter,W.N. (2001) Structure of Hjc, a Holliday junction resolvase, from *Sulfolobus solfataricus*. *Proc. Natl Acad. Sci. USA*, **98**, 5509–5514.
- Brünger,A.T. *et al.* (1998) Crystallography and NMR system: a new software suite for macromolecular structure determination. *Acta Crystallogr. D*, **54**, 905–921.
- CCP4 (1994) The CCP4 suite: programs for protein crystallography. *Acta Crystallogr. D*, **50**, 760–763.
- Constantinou,A., Davies,A.A. and West,S.C. (2001) Branch migration and Holliday junction resolution catalyzed by activities from mammalian cells. *Cell*, **104**, 259–268.
- Cox,M.M., Goodman,M.F., Kreuzer,K.N., Sherratt,D.J., Sandler,S.J. and Mariani,K.J. (2000) The importance of repairing stalled replication forks. *Nature*, **404**, 37–41.
- Doe,C.L., Osman,F., Dixon,J. and Whitby,M.C. (2000) The Holliday junction resolvase SpCCE1 prevents mitochondrial DNA aggregation in *Schizosaccharomyces pombe*. *Mol. Gen. Genet.*, **263**, 889–897.

- Duckett,D.R., Murchie,A.I., Giraud Panis,M.J., Pohler,J.R. and Lilley,D.M. (1995) Structure of the four-way DNA junction and its interaction with proteins. *Philos. Trans. R. Soc. Lond. B Biol. Sci.*, **347**, 27–36.
- Eggleston,A.K., Mitchell,A.H. and West,S.C. (1997) *In vitro* reconstitution of the late steps of genetic recombination in *E.coli*. *Cell*, **89**, 607–617.
- Ezekiel,U.R. and Zassenhaus,H.P. (1993) Localization of a cruciform cutting endonuclease to yeast mitochondria. *Mol. Gen. Genet.*, **240**, 414–418.
- Fogg,J.M., Schofield,M.J., Declais,A.C. and Lilley,D.M.J. (2000) Yeast resolving enzyme CCE1 makes sequential cleavages in DNA junctions within the lifetime of the complex. *Biochemistry*, **39**, 4082–4089.
- Garcia,A.D., Aravind,L., Koonin,E.V. and Moss,B. (2000) Bacterial-type DNA Holliday junction resolvases in eukaryotic viruses. *Proc. Natl Acad. Sci. USA*, **97**, 8926–8931.
- Hadden,J.M., Convery,M.A., Declais,A.C., Lilley,D.M.J. and Phillips,S.E.V. (2001) Crystal structure of the Holliday junction resolving enzyme T7 endonuclease I. *Nature Struct. Biol.*, **8**, 62–67.
- Hargreaves,D., Rice,D.W., Sedelnikova,S.E., Artymiuk,P.J., Lloyd,R.G. and Rafferty,J.B. (1998) Crystal structure of *E.coli* RuvA with bound DNA Holliday junction at 6 Å resolution. *Nature Struct. Biol.*, **5**, 441–446.
- Ichiyanagi,K., Iwasaki,H., Hishida,T. and Shinagawa,H. (1998) Mutational analysis on structure–function relationship of a Holliday junction specific endonuclease RuvC. *Genes Cells*, **3**, 575–586.
- Jones,T.A., Zou,J.Y., Cowan,S.W. and Kjeldgaard. (1991) Improved methods for binding protein models in electron density maps and the location of errors in these models. *Acta Crystallogr. A*, **47**, 110–119.
- Kowalczykowski,S.C. (2000) Initiation of genetic recombination and recombination-dependent replication. *Trends Biochem. Sci.*, **25**, 156–165.
- Kraulis,P.J. (1991) MOLSCRIPT—a program to produce both detailed and schematic plots of protein structures. *J. Appl. Crystallogr.*, **24**, 946–950.
- Kvaratskhelia,M., George,S.J., Cooper,A. and White,M.F. (1999) Quantitation of metal ion and DNA junction binding to the Holliday junction endonuclease Cce1. *Biochemistry*, **38**, 16613–16619.
- Laskowski,R.A., MacArthur,M.W., Moss,D.W. and Thornton,J.M. (1993) PROCHECK—a program to check the stereochemical quality of protein structures. *J. Appl. Crystallogr.*, **26**, 283–290.
- Lilley,D.M.J. and Norman,D.G. (1999) The Holliday junction is finally seen with crystal clarity. *Nature Struct. Biol.*, **6**, 897–899.
- Lilley,D.M.J. and White,M.F. (2000) Resolving the relationships of resolving enzymes. *Proc. Natl Acad. Sci. USA*, **97**, 9351–9353.
- Lilley,D.M.J. and White,M.F. (2001) The junction-resolving enzymes. *Nature Rev. Mol. Cell Biol.*, **2**, 433–443.
- Lockshon,D., Zweifel,S.G., Freeman-Cook,L.L., Lorimer,H.E., Brewer, B.J. and Fangman,W.L. (1995) A role for recombination junctions in the segregation of mitochondrial DNA in yeast. *Cell*, **81**, 947–955.
- Merrit,E.A. and Murphy,M.E.P. (1994) Raster3D version 2.0—a program for photorealistic molecular graphics. *Acta Crystallogr. D*, **50**, 869–873.
- Michel,B. (2000) Replication fork arrest and DNA recombination. *Trends Biochem. Sci.*, **25**, 173–178.
- Murzin,A.G., Brenner,S.E., Hubbard,T. and Chothia,C. (1995) SCOP: a structural classification of proteins database for the investigation of sequences and structures. *J. Mol. Biol.*, **247**, 536–540.
- Navaza,J. (1994) AmoRe—an automated package for molecular replacement. *Acta Crystallogr. A*, **50**, 157–163.
- Nicholls,A., Bharadwaj,R. and Honig,B. (1993) GRASP—graphical representation and analysis of surface properties. *Biophys. J.*, **64**, A116.
- Nishino,T., Komori,K., Tsuchiya,D., Ishino,Y. and Morikawa,K. (2001) Crystal structure of the archaeal Holliday junction resolvase Hjc and implications for DNA recognition. *Structure*, **9**, 197–204.
- Oram,M., Keeley,A. and Tsaneva,I.R. (1998) Holliday junction resolvase in *Schizosaccharomyces pombe* has identical endonuclease activity to the CCE1 homologue YDC2. *Nucleic Acids Res.*, **26**, 594–601.
- Orengo,C.A., Brown,N.P. and Taylor,W.R. (1992) Fast structure alignment for protein databank searching. *Proteins*, **14**, 139–167.
- Ortiz-Lombardia,M., Gonzalez,A., Eritja,R., Aymami,J., Azorin,F. and Coll,M. (1999) Crystal structure of a DNA Holliday junction. *Nature Struct. Biol.*, **6**, 913–917.
- Otwinowski,Z. and Minor,W. (1993) Oscillation data reduction program. In Sawyer,L., Isaacs,N. and Bailey,S. (eds), *Data Collection and Processing*. CLRC Daresbury Laboratory, Warrington, UK, pp. 556–562.
- Parsons,C.A. and West,S.C. (1988) Resolution of model Holliday junctions by yeast endonuclease is dependent upon homologous DNA sequences. *Cell*, **52**, 621–629.
- Parsons,C.A., Stasiak,A., Bennett,R.J. and West,S.C. (1995) Structure of a multisubunit complex that promotes DNA branch migration. *Nature*, **374**, 375–378.
- Pearl,F.M.G., Lee,D., Bray,J.E., Sillitoe,I., Todd,A.E., Harrison,A.P., Thornton,J.M. and Orengo,C.A. (2000) Assigning genomic sequences to CATH. *Nucleic Acids Res.*, **28**, 277–282.
- Piskur,J. (1997) The transmission disadvantage of yeast mitochondrial intergenic mutants is eliminated in the mgt1 (cce1) background. *J. Bacteriol.*, **179**, 5614–5617.
- Raaijmakers,H., Vix,O., Toro,I., Golz,S., Kemper,B. and Suck,D. (1999) X-ray structure of T4 endonuclease VII: a DNA junction resolvase with a novel fold and unusual domain-swapped dimer architecture. *EMBO J.*, **18**, 1447–1458.
- Roe,S.M., Barlow,T., Brown,T., Oram,M., Keeley,A., Tsaneva,I.R. and Pearl,L.H. (1998) Crystal structure of an octameric RuvA–Holliday junction complex. *Mol. Cell*, **2**, 361–372.
- Schofield,M.J., Lilley,D.M.J. and White,M.F. (1997) Sequence specificity of CCE1. *Biochem. Soc. Trans.*, **25**, S646–S646.
- Schofield,M.J., Lilley,D.M.J. and White,M.F. (1998) Dissection of the sequence specificity of the Holliday junction endonuclease CCE. *Biochemistry*, **37**, 7733–7740.
- Takahagi,M., Iwasaki,H. and Shinigawa,H. (1994) Structural requirements of substrate DNA for binding to and cleavage by RuvC, a Holliday junction resolvase. *J. Biol. Chem.*, **269**, 15132–15139.
- Terwilliger,T.C. (2000) Maximum-likelihood density modification. *Acta Crystallogr. D*, **56**, 965–972.
- Terwilliger,T.C. and Berendzen,J. (1999) Automated MAD and MIR structure solution. *Acta Crystallogr. D*, **55**, 849–861.
- Wardleworth,B.N., Kvaratskhelia,M. and White,M.F. (2000) Site-directed mutagenesis of the yeast resolving enzyme Cce1 reveals catalytic residues and relationship with the intron-splicing factor Mrs1. *J. Biol. Chem.*, **275**, 23725–23728.
- West,S.C. (1996) The RuvABC proteins and Holliday junction processing in *Escherichia coli*. *J. Bacteriol.*, **178**, 1237–1241.
- Whitby,M.C. and Dixon,J. (1997) A new Holliday junction resolving enzyme from *Schizosaccharomyces pombe* that is homologous to CCE1 from *Saccharomyces cerevisiae*. *J. Mol. Biol.*, **272**, 509–522.
- Whitby,M.C. and Dixon,J. (1998) Substrate specificity of the SpCCE1 Holliday junction resolvase of *Schizosaccharomyces pombe*. *J. Biol. Chem.*, **273**, 35063–35073.
- Whitby,M.C., Bolt,E.L., Chan,S.N. and Lloyd,R.G. (1996) Interactions between RuvA and RuvC at Holliday junctions: inhibition of junction cleavage and formation of a RuvA–RuvC–DNA complex. *J. Mol. Biol.*, **264**, 878–890.
- White,M.F. and Lilley,D.M. (1996) The structure-selectivity and sequence-preference of the junction-resolving enzyme CCE1 of *Saccharomyces cerevisiae*. *J. Mol. Biol.*, **257**, 330–341.
- White,M.F. and Lilley,D.M.J. (1997a) Characterization of a Holliday junction-resolving enzyme from *Schizosaccharomyces pombe*. *Mol. Cell Biol.*, **17**, 6465–6471.
- White,M.F. and Lilley,D.M.J. (1997b) The resolving enzyme CCE1 of yeast opens the structure of the four-way DNA junction. *J. Mol. Biol.*, **266**, 122–134.
- White,M.F. and Lilley,D.M.J. (1998) Interaction of the resolving enzyme YDC2 with the four-way DNA junction. *Nucleic Acids Res.*, **26**, 5609–5616.
- White,M.F., Giraud Panis,M.J.E., Pohler,J.R.G. and Lilley,D.M.J. (1997) Recognition and manipulation of branched DNA structure by junction-resolving enzymes. *J. Mol. Biol.*, **269**, 647–664.
- Zou,H. and Rothstein,R. (1997) Holliday junctions accumulate in replication mutants via a RecA homolog-independent mechanism. *Cell*, **90**, 87–96.
- Zweifel,S.G. and Fangman,W.L. (1991) A nuclear mutation reversing a biased transmission of yeast mitochondrial DNA. *Genetics*, **128**, 241–249.

Received September 6, 2001; revised and accepted October 12, 2001